Development of a digital droplet PCR approach for the quantification of soil micro-organisms involved in atmospheric CO 2 fixation

Marie Le Geay, Kyle Mayers, Martin Küttim, Béatrice Lauga, Vincent E J Jassey

Received: 5 March 2024 | Accepted: 23 May 2024

DOI: 10.1111/1462-2920.16666

BRIEF REPORT

ENVIRONMENTAL MICROBIOLOGY

Development of a digital droplet PCR approach for the quantification of soil micro-organisms involved in atmospheric CO_2 fixation

Marie Le Geay[1] | **Kyle Mayers**[2] | **Martin Küttim**[3] | **Béatrice Lauga**[4] | **Vincent E. J. Jassey**[1]

[1]Centre de Recherche sur la Biodiversité et l'Environnement (CRBE), Université de Toulouse, CNRE, IRD, Toulouse INP, Université Toulouse 3—Paul Sabatier (UT3), Toulouse, France

[2]NORCE Norwegian Research Centre AS, Bergen, Norway

[3]Institute of Ecology, School of Natural Sciences and Health, Tallinn University, Tallinn, Estonia

[4]Universite de Pau et des Pays de l'Adour, E2S UPPA, CNRS, IPREM, Pau, France

Correspondence
Marie Le Geay and Vincent E. J. Jassey, Centre de Recherche sur la Biodiversité et l'Environnement (CRBE), Université de Toulouse, CNRE, IRD, Toulouse INP, Université Toulouse 3—Paul Sabatier (UT3), Toulouse, France.
Email: marie.le-geay@univ-tlse3.fr; vincent.jassey@univ-tlse3.fr

Funding information
Agence Nationale de la Recherche, Grant/Award Numbers: EURTESS: ANR-18-EURE-0018; MIXOPEAT: ANR-17-CE01-0007; BALANCE: ANR-23-ERCC-0001-01

Abstract

Carbon-fixing micro-organisms (CFMs) play a pivotal role in soil carbon cycling, contributing to carbon uptake and sequestration through various metabolic pathways. Despite their importance, accurately quantifying the absolute abundance of these micro-organisms in soils has been challenging. This study used a digital droplet polymerase chain reaction (ddPCR) approach to measure the abundance of key and emerging CFMs pathways in fen and bog soils at different depths, ranging from 0 to 15 cm. We targeted total prokaryotes, oxygenic phototrophs, aerobic anoxygenic phototrophic bacteria and chemoautotrophs, optimizing the conditions to achieve absolute quantification of these genes. Our results revealed that oxygenic phototrophs were the most abundant CFMs, making up 15% of the total prokaryotic abundance. They were followed by chemoautotrophs at 10% and aerobic anoxygenic phototrophic bacteria at 9%. We observed higher gene concentrations in fen than in bog. There were also variations in depth, which differed between fen and bog for all genes. Our findings underscore the abundance of oxygenic phototrophs and chemoautotrophs in peatlands, challenging previous estimates that relied solely on oxygenic phototrophs for microbial carbon dioxide fixation assessments. Incorporating absolute gene quantification is essential for a comprehensive understanding of microbial contributions to soil processes. This approach sheds light on the complex mechanisms of soil functioning in peatlands.

INTRODUCTION

Carbon fixing micro-organisms (CFMs) are key drivers of the carbon (C) cycle as they assimilate atmospheric CO_2 and contribute to the soil organic C sequestration (Ge et al., 2013; Liu et al., 2018; Yuan et al., 2012). CFMs fix CO_2 through seven major metabolic pathways, namely, the reductive pentose phosphate cycle (also known as Calvin–Benson–Bassham, CBB cycle), the reductive citrate cycle (rTCA cycle), the 3-hydroxypropionate bi-cycle (3-HP cycle), the 3-hydroxypropionate/4-hydroxybutyrate cycle (3-HP/4-HB cycle), the dicarboxylate-hydroxybutyrate cycle (DC/4-HB cycle), the reductive acetyl-CoA pathway (also known as Wood–Ljungdahl pathway) and the reductive glycine pathway (Berg, 2011; Figueroa et al., 2018; Sánchez-Andrea et al., 2020; Huang et al., 2022). The CBB cycle is the predominant pathway utilized by micro-organisms in soils (Bay et al., 2021). It is present across different taxonomic levels (bacteria and protists), notably in green algae, diatoms, cyanobacteria and aerobic bacteria

(Berg, 2011; Yuan et al., 2012). Oxygenic phototrophs and chemoautotrophs are two major CFMs using the CBB cycle to fix atmospheric CO_2. Oxygenic phototrophs derive their energy from light to assimilate CO_2 through photosynthesis, whereas chemoautotrophs use reduced chemical compounds such as sulfur compounds, molecular hydrogen and reduced metals to assimilate CO_2 (Hügler & Sievert, 2011). Potential CO_2 fixation through the CBB cycle also recently emerged in aerobic anoxygenic phototrophic bacteria (AAnPBs). Recent studies found AAnPB strains possessing (and expressing) genes of the CBB cycle (Graham et al., 2018; Tang et al., 2021). Even though CFMs are now well recognized for their role in autotrophic CO_2 fixation in soils, their absolute quantification remains elusive (Liao et al., 2023). As microbial CO_2 assimilation rates are closely linked to CFMs abundance (Hamard, Céréghino, et al., 2021; Hamard, Küttim, et al., 2021; Liao et al., 2023), it is essential to provide absolute quantification of these micro-organisms in soils to better assess their contribution to C fixation in terrestrial ecosystems.

Quantification of micro-organisms can be laborious notably in complex matrices such as soils. Numerous approaches are available with their own strengths and flaws (Wang, Howe, et al., 2021). Methods based on cell counts such as fluorescence microscopy or flow cytometry have been widely used (Bressan et al., 2015; Frossard et al., 2016), as well as methods based on adenosine triphosphate quantification (Hammes et al., 2010; Karl, 1980) or phospholipids fatty acids analysis (PLFA, Frostegård & Bååth, 1996). However, these methods (except PLFA) do not allow differentiation between different bacterial groups. Since the development of Polymerase Chain Reaction (PCR, Mullis et al., 1986), different molecular approaches, such as real-time PCR (qPCR, Higuchi et al., 1993), digital PCR (dPCR, Vogelstein & Kinzler, 1999) including digital droplet polymerase chain reaction (ddPCR) (Hindson et al., 2011) have emerged to count either total bacteria (using primers targeting the 16S rRNA gene) or specific populations of bacteria and their associated functions (using primers targeting specific genes; Figure A1). The qPCR is based on the monitoring of the amplification after each PCR cycle by using a fluorescent probe or dye (Higuchi et al., 1993; Hou et al., 2023; Pinheiro et al., 2012). However, this method requires external calibration and normalization with endogenous controls (Hindson et al., 2011). It is also sensitive to inhibitors and to the initial amount of the target since low concentrations will hardly be detected (Hindson et al., 2011; Hou et al., 2023; Pinheiro et al., 2012; Taylor et al., 2017). The ddPCR method uses a simple microfluidic circuit and surfactant chemistry to divide the reaction mixture into approximately 20,000 partitioned water-in-oil droplets. These droplets can either contain the target molecule or not. After being amplified with a fluorescent probe or labelling dye, it is possible to discriminate between positive and negative droplets. The concentration of the target molecule is then calculated based on Poisson distribution: $\lambda = -\ln(1-p)$, where λ is the average number of target molecules per replicate reaction and p is the fraction of positive end-point reactions. Calculations of the final target DNA concentration are done using λ, the volume of each replicate and the number of replicates (see Hindson et al., 2011). Several studies have compared qPCR and ddPCR and found that ddPCR had better precision, repeatability, sensitivity and stability than qPCR (Taylor et al., 2017; Wang et al., 2022; Xue et al., 2018; Zhao et al., 2016). Nowadays, ddPCR is increasingly used in environmental studies (see Hou et al., 2023 for a complete review), even though several challenges are faced and require appropriate optimization of ddPCR parameters (see Kokkoris et al., 2021). Adjusting many factors related to the PCR reaction, including the concentration of template DNA, thermocycling conditions and the threshold setting used to discriminate positive and negative droplets, can notably influence the detection of target DNA from environmental samples (Kokkoris et al., 2021; Rowlands et al., 2019; Witte et al., 2016).

In this study, we aim to provide absolute quantification of the main (oxygenic phototrophs and chemoautotrophs) and emerging (AAnPBs) CFMs in peatlands. As peatlands are a major C reservoir (Nichols & Peteet, 2019), quantifying the main CFMs will enhance our understanding of peatland C cycling. More precisely, we aimed to (1) optimize ddPCR conditions to enumerate total prokaryotes and specific groups of CFMs (oxygenic phototrophs, chemoautotrophs and AAnPBs), (2) apply optimized ddPCR to target CFMs in two peatland types (moderately rich fen and open bog) and (3) at different depths (0–15 cm). As protists are very abundant in peatlands, we hypothesize that oxygenic phototrophs, (which can be found among bacteria and protists), will be the most abundant CFMs in peatlands while chemoautotrophs and AAnPBs will be rare community members. We also forecast that CFMs absolute abundance will differ between the bog and the fen as these two peatland habitats harbour different biotic and abiotic factors. We further hypothesized that oxygenic phototrophs and AAnPBs will be less abundant with depth as the amount of light decreases, thus favouring chemoautotrophs.

EXPERIMENTAL PROCEDURE

Sampling and DNA extraction

Peat samples were collected in two peatlands, Counozouls (France) and Männikjärve (Estonia). Counozouls mire is located in the French Pyrenees mountains

(42°41′16 N″–2°14′18″ E—1.374 m a.s.l). It is a moderately rich fen belonging to the Special Area of the Natura 2000 Conservation site 'Massif du Madres Coronat'. The peatland of Männikjärve is an open bog located in the Endla mire system in Central Estonia (58°52′26.4″ N–26°15′03.6″ E—82 m a.s.l). In both sites, the water level was below 20 cm, so all samples were above the water level during sampling. At both sites, we collected three cores from similar and homogeneous habitat—*Sphagnum* lawn—by cutting peat soil for DNA analysis. Also, we sampled pore water to conduct chemical analysis. Then, the cores were cut into three depths corresponding to the living layer (D1; 0–5 cm), the decaying layer (D2; 5–10 cm) and the dead layer (D3; 10–15 cm) based on *Sphagnum* shoots (Figure A2). At each depth, a few grams of peat were collected, cut into small pieces, homogenized and placed in sterile 5 mL Eppendorf tubes containing 3 mL of RNA*later* (ThermoFisher). The tubes were stored at −20°C upon our arrival in the laboratory. DNA was extracted using the DNeasy PowerSoil Pro Kit (Qiagen) following the manufacturer's instructions. After the elution of DNA (70 μL in the final solution), DNA concentration was quantified using a Nanodrop ND-1000 spectrophotometer. Extracts were then stored at −20°C before DNA amplification.

Vegetation, climate and chemical characterization of each site

For both sites, we extracted bioclimatic data from weather stations located on-site for the time period where the samples were collected (i.e., June, July and August mean air temperatures [JJA Temp] and total precipitations [JJA Prec]). We also collected pore water in each plot and filtered it with Whatman filters (1 μm pore size). In the laboratory, we analysed several parameters including pH, dissolved organic carbon (DOC) and total nitrogen (DTN). DOC and DTN were measured by combustion on a Shimadzu TOC-L. The vegetation cover (VP cover) of each plot was retrieved from a former vegetation survey (Sytiuk, Céréghino, Hamard, Delarue, Dorrepaal, et al., 2022). Briefly, high-resolution photographs were taken in each half of the plot. Then, we followed Buttler et al. (2015) to analyse the pictures and estimate the cover of each species. Vegetation cover, climatic and chemical parameters are available in Table A1.

Primer choice and design

The total concentration of prokaryotes was obtained by targeting the 16S rRNA gene. Micro-organisms involved in oxygenic photosynthesis were quantified using the 23S rRNA gene while chemoautotrophs were quantified using the *cbbL* gene that encodes the large subunit of RuBisCO form IA (Alfreider & Bogensperger, 2018; Kusian & Bowien, 1997). Chemoautotrophs are widespread and forms IA, IC and II of the RuBisCO can be found, however, form IA is the prevalent form allowing a broad diversity of chemoautotrophs (Shively et al., 1998). For AAnPBs, we used the *pufM* gene that encodes for the M subunit of the type II photochemical reaction centre (Achenbach et al., 2001; Béjà et al., 2002). This gene is often chosen to target AAnPBs as it is universally distributed among AAnPBs allowing it to target purple sulfur and non-sulfur phototrophs, Chloroflexi but not cyanobacteria (Achenbach et al., 2001; Béjà et al., 2002). To select the primers, we first searched the literature and identified primer pairs that have been already used either in ddPCR or in qPCR. We used the primer pairs L/Prba338f and K/Prun518r for prokaryotes (Øvreås et al., 1997), cbbLR1F/cbbLR1inR for chemoautotrophs (Selesi et al., 2007) and pufMforward557/pufMreverse750 for AAnPBs (Table 1; Du et al., 2006). However, we could not find suitable primers matching a short region of the 23S rRNA gene targeting oxygenic phototrophs with satisfying length and degeneracies. Therefore, we designed a new set of primers for ddPCR.

To do so, we first conducted a PCR on peat samples to target the 23S rRNA gene using the existing primers P23SrV-f1 with P23SRV-r1 (Sherwood & Presting, 2007) and sequenced PCR amplicons. The PCR programme was run in a total volume of 50 μL containing 25 μL of AmpliTaq Gold™ Master Mix (Applied Biosystems, ThermoFisher), 19 μL of ultrapure water, 1 μL of forward and 1 μL of reverse primer (final concentration of 20 μM) and 4 μL of DNA template. The PCR reaction conditions included an initialization step of 10 min at 95°C followed by 35 cycles of 1 min at 94°C, 45 s at 55°C, 45 s at 72°C and a final extension step of 10 min at 72°C. PCR quality was assessed using 1.65% agarose gel electrophoresis. The high throughput sequencing was performed by the GeT-PlaGe platform (Genotoul, Toulouse, France) using Illumina MiSeq v3 technology. Based on the results of the sequencing, we designed for this study the new forward primer 23S255f to target a short region of the 23S rRNA gene as follows. We aligned all the sequences obtained from sequencing using Clustal Omega (EMBL-EBI) and blasted (nBLAST with NCBI) these sequences to ensure that they corresponded to the *23S rRNA* gene. Then, using BioEdit v5.0.9, we generated a consensus sequence based on the aligned sequences (Figure A3). We searched in this consensus sequence for a conserved region and checked every degenerated base to create a manually curated sequence. We examined if this sequence matched the guidelines for q/dPCR (Rodríguez et al., 2015) (amplicon length <250 pb, GC content of 50%–60%, annealing temperature of 50–65°C, no secondary structure and

TABLE 1 Primer pairs used in this study.

Micro-organisms targeted	Primers	Amplicon size	Primer sequence	Reference
Prokaryotes	L/Prba338f	180 bp	5′-ACT CCT ACG GGA GGC AGC AG-3′	(Øvreås et al., 1997)
	K/Prun518r		5′-ATT ACC GCG GCT GCT GG-3′	
Oxygenic phototrophs	23S255f	160 bp	5′-GGA TTA GAT ACC CYD GTA GTC C-3′	This study
	P23SrV_r1		5′-TCA GCC TGT TAT CCC TAG AG-3′	(Sherwood & Presting, 2007)
Chemoautotrophs	cbbLR1F	274 bp	5′-AAG GAY GAC GAG AAC ATC-3′	(Selesi et al., 2007)
	cbbLRintR		5′-TGC AGS ATC ATG TCR TT-3′	
AAnPBs	pufM forward 557	193 bp	5′-TAC GGS AAC CTG TWC TAC-3′	(Du et al., 2006)
	pufM reverse 750		5′-CCA TSG TCC AGC GCC AGA A-3′	

Abbreviation: AAnPBs, aerobic anoxygenic phototrophic bacteria.

primer-dimer, no repetition of Gs and Cs longer than 3 bases, Table A2) and finally obtained the new forward primer 23S255f: 5′-GGA TTA GAT ACC CYD GTA GTC C-3′. By using the new primer set, the forward primer 23S255f with the reverse primer P23SRV-r1 (∼160 pb), we targeted oxygenic phototrophs.

To check for primers' specificity and coverage, we conducted PCRs on our samples using the same primers used for ddPCR (Table 1). PCRs were performed in a total volume of 50 μL containing 25 μL of AmpliTaq Gold™ Master Mix (Applied Biosystem, ThermoFisher), 19 μL of ultrapure water, 1 μL of forward and 1 μL of reverse primer (final concentration of 20 μM) and 4 μL of DNA template according to initial DNA concentration. The PCR reaction conditions can be found in Table A3. PCR quality was assessed using 1.65% agarose gel electrophoresis. The high throughput sequencing was performed by the GeT-PlaGe platform (Genotoul, Toulouse, France) using Illumina MiSeq technology with the *V3 chemistry*. *For the 23S rRNA gene, ASVs taxonomy was assigned using microgreen-db algae v1.2* (Djemiel et al., 2020) *and SILVA v138.1* (Quast et al., 2013), *for cbbL and pufM sequences were aligned, clustered* at 95% and taxonomy was assigned using BLASTn (NCBI). Based on these results we classified retrieved ASVs as belonging to the right group or not and calculated the percentage of each group (Figure A4A–C). The results showed that for each gene, more than 80% of the ASVs belonged to the targeted functional group (Figure A4). This highlights that the primers chosen allowed to target specifically oxygenic phototrophs, chemoautotrophs and AAnPBs, respectively, while ensuring both good coverage and specificity.

ddPCR conditions

The absolute abundance of genes was measured using digital droplet PCR (ddPCR, BioRad). The ddPCR reactions were run in a total volume of 20 μL on a DX200 instrument (BioRad) with 10 μL of EvaGreen Supermix (BioRad, 1X), 0.5 or 0.3 μL of each primer (final concentration 250 or 150 nM respectively) and 4 or 4.4 μL of ultrapure water. Template DNA (5 μL) diluted at 10, 100 or 1,000 times was added to the reaction mix. This mixture was then emulsified with QX200 Droplet Generation Oil for EvaGreen (BioRad) using the QX200 Droplet Generator (BioRad) and was manually transferred into a 96-well PCR plate. The plate was heat-sealed with a foil seal and then placed on a C1000 Touch Thermocycler with a deep-well module (BioRad) to run the PCR using different programmes (see the section 'ddPCR optimization' for more details). Following amplification, plates were equilibrated for at least 10 min at room temperature. Then, plates were loaded on a QX200 Droplet Reader (BioRad) and the fluorescence was read and analysed using QuantaSoft software. Thresholds for positive and negative droplets were manually defined using ultrapure water as a negative control and DNA extracted from different cultures of micro-organisms as positive and negative controls. *Escherichia coli* DNA diluted 1/100 was used as a positive control for prokaryotes and as a negative control for the other genes. *Micromonas pusilla* (a micro-algae) DNA diluted 1/100 was used as a positive control for oxygenic phototrophs. QuantaSoft provides a final concentration of target copies·μL^{-1} of ddPCR reaction. For each sample, final gene concentration was obtained by taking into account the volume of ddPCR reaction mixture (20 μL), the concentration of template DNA added to reaction mixture (5 μL), the dilution factor of the template DNA (10, 100 or 1,000), the volume of DNA obtained at the end of extraction and finally, we normalized the DNA concentration of the extract by the amount of dry peat used for each extraction to obtain a final concentration in target copies·g^{-1} of dry peat (copies·g^{-1} DW).

TABLE 2 Optimized digital droplet polymerase chain reaction (ddPCR) parameters including primer concentrations, DNA template dilution, optimal annealing temperature, ddPCR thermocycling conditions and positive and negative controls.

Primers	L/Prba338f with K/Prun518r	23S255f/P23Srv-r1	cbbLR1F/cbbLRintR1	pufMfwd557/pufMrev750
Gene targeted	16S rRNA	23S rRNA	*cbbL*	*pufM*
Primers concentration	150 nM	250 nM	250 nM	250 nM
DNA dilution	1/1000	1/100 (D1, D2) and 1/10 (D3)	1/10	1/100 (D1, D2) and 1/10 (D3)
Annealing temperature	61°C	57.6°C	53°C	50.2°C
ddPCR conditions	98°C—5 min	98°C—5 min	98°C—5 min	98°C—5 min
	40 cycles	40 cycles	45 cycles	45 cycles
	94°C—30 s	94°C—30 s	94°C—1 min	94°C—1 min
	61°C—1 min	57.6°C—1 min	53°C—2 min	50.2°C—2 min
	4°C—5 min	4°C—5 min	4°C—5 min	4°C—5 min
	98°C—10 min	98°C—10 min	98°C—10 min	98°C—10 min
	Ramp rate = 2°C/s	Ramp rate = 2°C/s	Ramp rate = 1°C/s	Ramp rate = 1°C/s
Positive control	*E. coli* DNA (diluted 1/100)	*M. pusilla* DNA (diluted 1/100)	/	/
Negative control	UPW	*E. coli* DNA (diluted 1/100) UPW	*E. coli* DNA (diluted 1/100) UPW	*E. coli* DNA (diluted 1/100) UPW

Abbreviation: UPW, ultra-pure water.

ddPCR optimization

For all the assays, we tested two primer concentrations (150 and 250 nM); a temperature gradient based on the theoretical annealing temperature of the primers; different dilutions of the template (1/10, 1/100 and 1/1,000) and different species DNA to find controls (*E. coli*, *M. pusilla*). We defined thermocycling conditions as 98°C for 5 min followed by 40 cycles of 94°C for 30 s, different temperatures or gradient of temperature for 30 s, followed by 5 min at 4°C and 98°C for 10 min. The ramp rate was set up at 2°C/s. When required, these parameters were adjusted to optimize the assays. For two assays (16S and 23S rRNA genes) we used the following PCR conditions: 98°C for 5 min followed by 40 cycles of 94°C for 30 s, 61 and 57.6°C for 1 min, followed by 5 min at 4 and 98°C for 10 min with a ramp rate of 2°C/s and the others (*cbbL* and *pufM* genes) we used: 98°C for 5 min followed by 45 cycles of 94°C for 1 min, 53 and 50.2°C for 2 min, followed by 5 min at 4 and 98°C for 10 min with a ramp rate of 1°C/s (Table 2).

Statistical analyses

Data were visually checked and tested for normality and homoscedasticity and log-transformed when necessary. Normality was assessed using the Shapiro–Wilk test (Shapiro & Wilk, 1965). To see if the gene concentrations differed according to location or depth we conducted a one-way ANOVA. We also tested if the concentration significantly differed according to the gene targeted. The post hoc test (Tukey honestly significant difference test) was further applied when a significant difference was found between location, depth and genes (Keselman & Rogan, 1977). We tested the effect of environmental parameters (including pH, DOC, DTN, VP cover, JAA Temp and JAA Prec) on gene abundance using linear mixed-effects models (LME) using the R package LME4 v1.1-35.3. We first standardize our environmental dataset using the function *decostand* of the R package vegan v2.6-4. As our environmental data were highly colinear, our models were fitted using only pH, nutrient (DTN), climate and vegetation (VP cover) as fixed effects and site as a random effect. We used the VIF (variance inflation factor) value to select the variables included in the model. Finally, we performed variance partitioning using the function *partR2* of the R package partR2 v0.9.2.

Statistical analyses were performed using RStudio v12.0 (RStudio Team, 2020) with R build under v4.3.2 and graphical representations were done using ggplot2 v3.4.0 (Wickham, 2016).

RESULTS AND DISCUSSION

Optimized ddPCR succeeded in amplifying universal and specific genes from peat samples

We tested different ddPCR conditions to obtain both a good amplification of the target genes and a separation

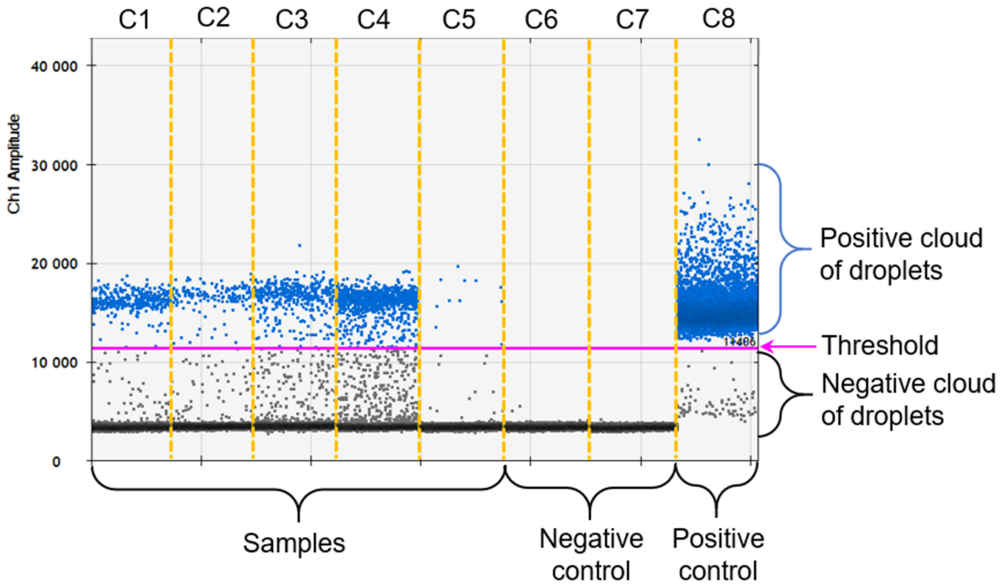

FIGURE 1 Example of results of digital droplet polymerase chain reaction (ddPCR) obtained for the 23S rRNA gene after analysis of raw data with QuantaSoft software. C1–C5 = soil samples, C6 = ultrapure water (negative control), C7 = *E. coli* DNA (corresponding here to a negative control) and C8 = *M. pusilla* DNA (positive control). Horizontal purple line corresponds to the threshold manually set thanks to negative and positive controls. Blue dots correspond to positive droplets (containing target DNA) and black dots to negative droplets (not containing target DNA).

between positive and negative clouds of droplets (Figure 1). When numerous droplets were present without a clear separation (rain), ddPCR conditions were optimized (Figures A5–A8) following recommendations from previous studies (Kokkoris et al., 2021; Rowlands et al., 2019; Witte et al., 2016). We notably optimized both primers' concentrations and annealing temperatures. Optimizing these two primer parameters directly impacted the separation of clouds of positive and negative droplets. Usually, a primer concentration of 250 nM provides a better separation of clusters of droplets, but for the 16S rRNA gene, we found a better separation for 150 nM, probably because it decreased the fluorescence level (better for a gene with high occurrence). We also optimized the dilution of the target DNA as it ensures both, dilution of potential inhibitors and avoidance of the saturation of the system with excessive number of positive droplets and absence of negative droplets (Figure A5 well A05). We also changed the thermocycling conditions by increasing the number of cycles, the denaturation, annealing and elongation times which improved already the separation of the clusters. To obtain an even better separation between positive and negative droplets we decreased the ramp rate which led to compact and well-separated clouds of positive and negative droplets. Eventually, we used positive and negative controls to set appropriate thresholds (Demeke et al., 2021; Kokkoris et al., 2021; Rowlands et al., 2019; Witte et al., 2016). Results of the optimization are presented in Table 2 and Figures A5–A8.

Once the assays were optimized, we used the ddPCR parameters defined to amplify DNA from samples of the two peatland locations (Table 2). We retrieved 16S rRNA gene concentrations of 10.3 ± 2.76 × 10^6 copies g^{-1} DW in Counozouls and 2.11 ± 0.21 × 10^6 copies g^{-1} DW in Männikjärve. Previous peatland studies found total bacterial concentrations from 1 × 10^6 copies g^{-1} DW or copies·mL^{-1} (Gilbert et al., 1998; Lew et al., 2016) to 1 × 10^{10} copies g^{-1} DW or copies·mL^{-1} (Lin et al., 2012; Wen et al., 2018) which is consistent with our findings. Our data further showed that CFM gene concentrations were very similar (p >0.05, ANOVAs; Figure 2). Average 23S rRNA gene concentration was 14.0 ± 2.62 × 10^5 copies g^{-1} DW in Counozouls and 6.98 ± 1.67 × 10^5 copies·g^{-1} DW in Männikjärve. Again, this is consistent with other findings from soils (Jassey et al., 2022) and in particular, peatlands where concentrations around 1 × 10^5–10^{-6} copies g^{-1} DW have been found using microscopy and qPCR (Gilbert et al., 1998; Jassey et al., 2015; Reczuga et al., 2018; Tang et al., 2018). On average, *cbbL* gene concentration was 9.90 ± 2.36 × 10^5 copies g^{-1} DW in Counozouls and 2.57 ± 0.43 × 10^5 copies g^{-1} DW in Männikjärve. Similar abundances were retrieved in soils using qPCR (Keshri et al., 2015; Wang, Li, et al., 2021; Xiao et al., 2014; Yin et al., 2022). For the *pufM* gene, 8.17 ± 1.59 × 10^5 copies g^{-1} DW were retrieved in Counozouls and 3.24 ± 0.61 × 10^5 copies g^{-1} DW in Männikjärve. Again, these concentrations were comparable to AAnPBs concentrations found in soils (1–

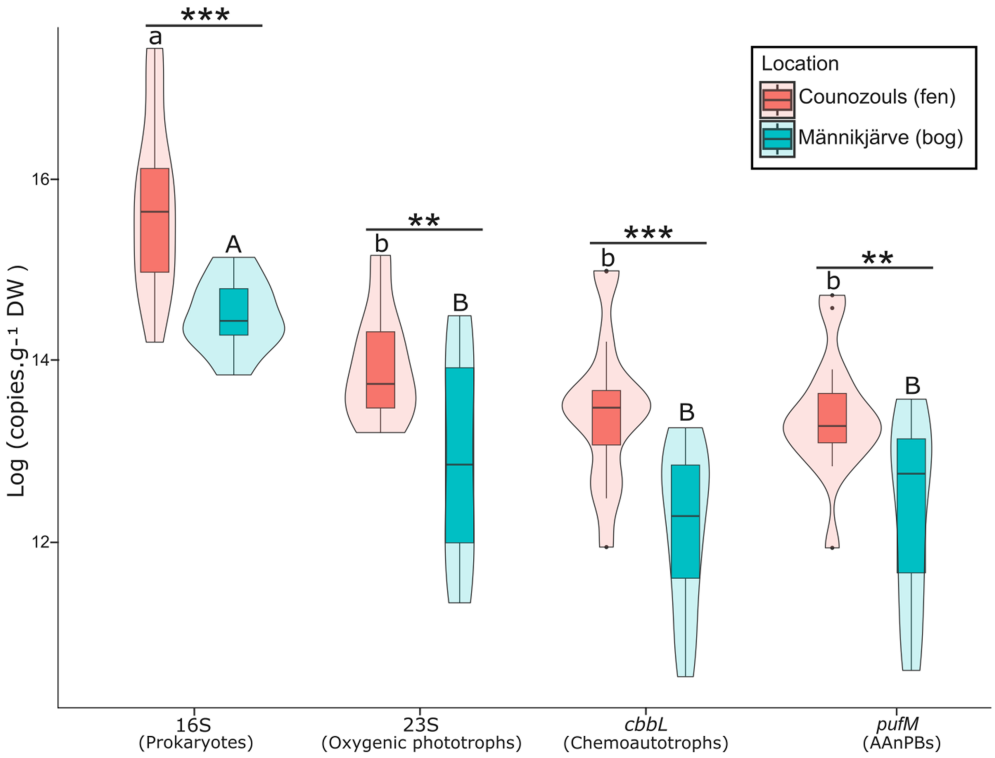

FIGURE 2 Absolute quantification of 16S rRNA gene targeting prokaryotes, 23S rRNA gene targeting oxygenic phototrophs, *cbbL* targeting chemoautotrophs and *pufM* targeting aerobic anoxygenic phototrophic bacteria (average of all depths) in Counozouls (fen) and Männikjärve (bog). Boxplots represent the logarithm of the total gene copies·g^{-1} DW and violin plots show the shape of data distribution. The horizontal black line in the box corresponds to the median and the edges of the box to 1st and 3rd quartiles. The vertical black line on the top and bottom of the boxplot represent respectively the highest and lowest values in the ±1.5 interquartile range. Black dots correspond to the outliers. Lowercase and uppercase letters represent the statistical difference between genes in Counozouls and Männikjärve, respectively. Horizontal bars with * represent the statistical difference between peatlands (Counozouls and Männikjärve) for each gene, **p <0.01; ***p <0.001. $n = 15$ for each gene at each location.

50×10^5 copies g^{-1}) or in aquatic environments (6×10^4–12×10^5 copies mL^{-1}) (Lew et al., 2016; Sato-Takabe et al., 2016, 2020; Tang et al., 2018). Altogether, these results showed that ddPCR is a suitable and reliable method to quantify absolute gene concentrations from complex soil matrices, like peat. Indeed, peat samples are usually rich in humic substances that are hardly removed during DNA extraction (Delarue et al., 2011). Their presence in DNA samples can inhibit Taq DNA polymerase and the fluorescence signal of double-stranded DNA binding dyes (Sidstedt et al., 2015). By optimizing ddPCR parameters we were able to overcome this potential issue and improve the separation between positive and negative droplets.

The abundance of CFMs differs between fen and bog and with depth

Overall, we found that gene concentrations in the fen were up to 4 times greater than gene concentrations in the bog (p <0.05 for all genes, ANOVAs; Figure 2). This pattern agrees with previous findings on total bacteria (Lin et al., 2012; Mpamah et al., 2017; Xu et al., 2021) and photoautotrophic bacteria (Hamard, Céréghino, et al., 2021; Sytiuk, Céréghino, Hamard, Delarue, Guittet, et al., 2022) abundances assessed by either inverted microscopy, flow cytometry or PLFA assays. As a moderately rich fen and an open bog, Counozouls and Männikjärve present different climatic conditions, nutrient contents, acidity and vegetation cover (Table A1; Sytiuk, Céréghino, Hamard, Delarue, Guittet, et al., 2022). To assess the effect of these environmental parameters on microbial gene abundance we conducted linear mixed effect models (Table A8) and performed a variance partitioning (Figure 3A–D). Our results highlight that climate and vegetation best explained the abundance of 23S rRNA, *cbbL* and *pufM* genes (Figure 3B–D) while the abundance of the 16S rRNA gene was mainly explained by pH and climate and vegetation cover (Figure 3). This finding corroborates previous findings on microbial CO_2 fixation in soils, where nutrient and water content (Guo et al., 2015; Zhao et al., 2021), soil pH and soil organic carbon (SOC) (Lew et al., 2016; Lin et al., 2012; Nowak et al., 2015; Zhao et al., 2021) have been shown to influence microbial abundance in general and microbial CO_2 fixation in particular. Moreover, Counozouls

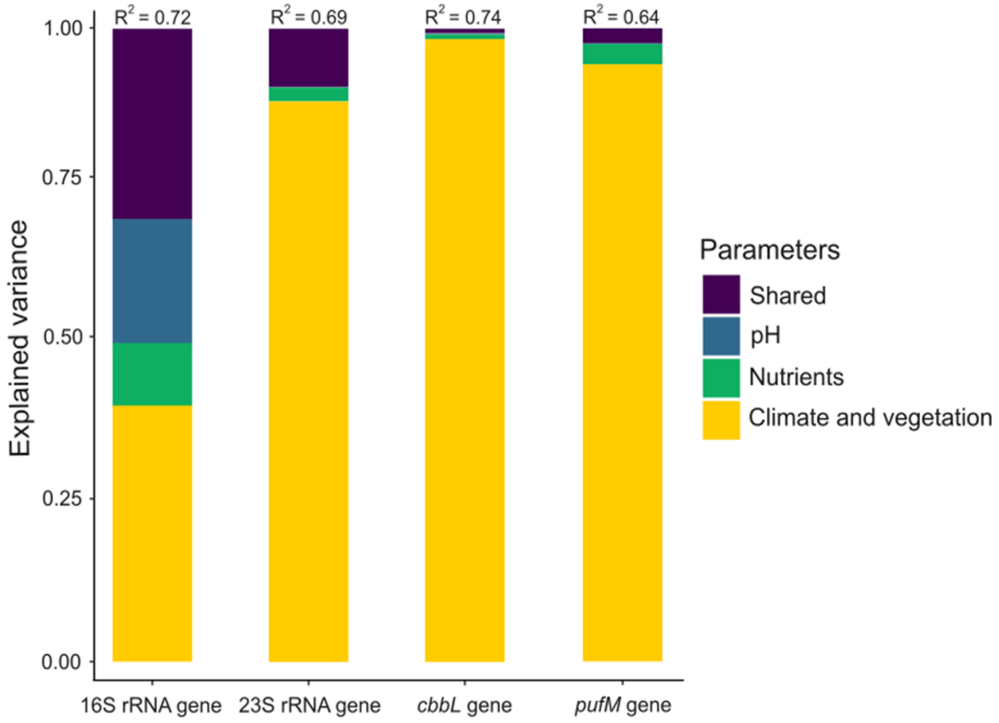

FIGURE 3 Variance partitioning evaluating the unique and shared portions explained by pH, nutrient, climate and vegetation on 16S rRNA, 23S rRNA, *cbbL* and *pufM* genes. Shared corresponds to the percent of variance explained by all predictors.

presented warmer and wetter conditions than Männikjärve which may have increased the abundance of CFMs as previously shown for peatlands microbes (Le Geay et al., 2024), but also for microbial biomass in soils (Xu et al., 2013; Yuan et al., 2012). Although other environmental drivers of CFM abundance in peatlands still need to be identified, our results suggest that complex interactions between climate, peat properties and vegetation cover determine CFM abundance in peatlands. Alternatively, DNA found in peat can be a mix of DNA from active cells, dead cells or even extracellular DNA (Pearman et al., 2022), which could explain the observed high abundance in the fen. As pH is more acidic in Männikjärve than in Counozouls (respectively 5.01 and 5.8), it could have favoured DNA degradation in Männikjärve whereas physico-chemical conditions found in Counozouls may better preserve the DNA letting both active and dead cells be preserved. More site comparisons will be required in the future to further understand this observed pattern.

In addition to the peatland type effect, our data evidenced a net depth effect but with opposite patterns between the fen and the bog (Figure 4). In Counozouls, all gene concentrations aside from 23S rRNA and *pufM* increased with depth (p <0.05, ANOVAs; Figure 4; Tables A4–A8) while in Männikjärve, all gene concentrations but 16S rRNA decreased with depth (p <0.05, ANOVAs; Figure 4; Tables A4–A8). More particularly, we found that the concentration of the 23S rRNA gene did not vary with depth (p >0.05) except between D2 and D3 samples in Counozouls (p <0.05; Figure 4; Table A5), while it gradually decreased with depth in Männikjärve (p <0.001; Figure 4; Table A5). As oxygenic phototroph biomass is tightly linked to light availability (Bengtsson et al., 2018), we were expecting such a decrease in the 23S rRNA gene with depth. We tentatively explain the high abundance of the 23S rRNA gene with depth in Counozouls by the dominance of cyanobacteria in the oxygenic phototrophic community (Figure A9A,B). Indeed, cyanobacteria can capture light at low intensities thanks to highly adaptable ecophysiological traits (Carey et al., 2012) and could therefore remain abundant with depths in Counozouls.

The concentration of the *cbbL* gene targeting chemoautotrophs significantly increased with depth in Counozouls (p <0.05, ANOVA), whereas it significantly decreased with depth in Männikjärve (p <0.001; ANOVA; Figure 4; Table A6). Chemoautotrophs are notably studied in deep sea vents, coastal sediments and soils, where reduced compounds such as sulfur compounds, molecular hydrogen and reduced metals are particularly abundant and facilitate chemoautotrophy (Boschker et al., 2014; Gomez-Saez et al., 2017; Nakagawa & Takai, 2008; Wang et al., 2023; Yang et al., 2017). We found that chemoautotrophs were more abundant in the surface samples in Männikjärve but not in Counozouls. This suggests that geochemical conditions as well as reduced compound availability

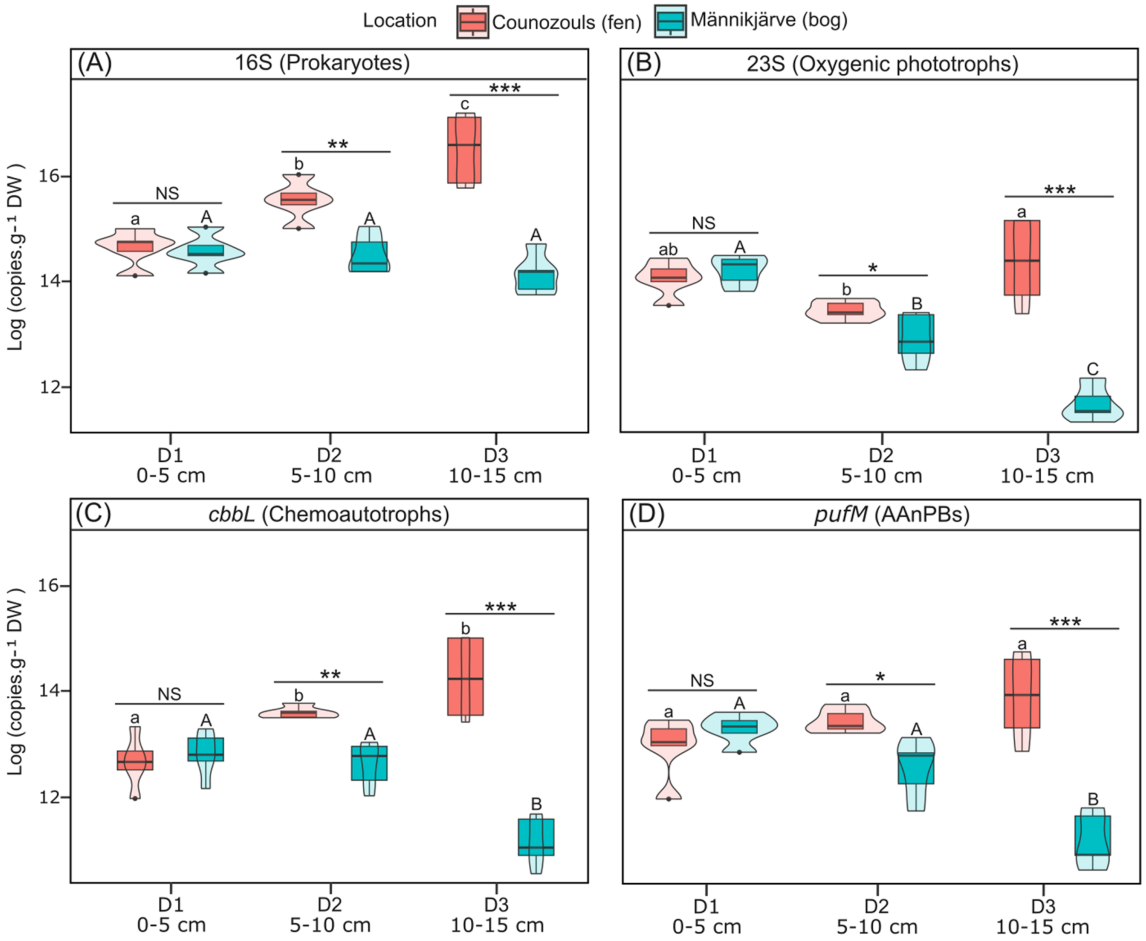

FIGURE 4 Absolute quantification of (A) 16S rRNA gene targeting prokaryotes, (B) 23S rRNA gene targeting oxygenic phototrophs, (C) *cbbL* targeting chemoautotrophs and (D) *pufM* targeting aerobic anoxygenic phototrophic bacteria (AAnPBs) at different depths in Counozouls (fen) and Männikjärve (bog). Boxplots represent the logarithm of the total gene copies·g^{-1} DW and violin plots show the shape of data distribution. The black line in the box corresponds to the median and the edges of the box to 1st and 3rd quartiles. The vertical black line on the top and bottom of the boxplot represent respectively the highest and lowest values in the ±1.5 interquartile range. Black dots correspond to the outliers. Lowercase and uppercase letters represent the statistical difference between genes in Counozouls and Männikjärve, respectively. Horizontal bars with * represent the statistical difference between peatlands (Counozouls and Männikjärve) at each depth. NS, not significant (p >0.05); *p <0.05; **p <0.01; ***p <0.001. $n = 5$ for each microbial group at each depth for each location. D1 (0–5 cm) corresponds to the living layer, D2 (5–10 cm) to the decaying layer and D3 (10–15 cm) to the dead layer.

might be more limiting in Männikjärve than in Counozouls. For the *pufM* gene that targets AAnPBs, we did not see a significant difference in gene concentrations between depths in Counozouls (p >0.05). In Männikjärve we found a significant decrease in the *pufM* gene concentration with depth (p <0.001; ANOVA; Figure 4; Table A7). Being obligate aerobic micro-organisms, AAnPBs have mainly been found in the euphotic zone of aquatic systems (Koblížek et al., 2003). They are often described as a highly active part of microbial communities; however, we lack information regarding their importance in soil communities as well as their metabolic capacities with only a few studies working on AAnPBs in soils (Feng et al., 2011; Tang et al., 2018). Our data show that AAnPBs are more abundant in fens than in bogs, suggesting they could play an important ecological role in these ecosystems.

Ratios of oxygenic phototrophs, chemoautotrophs and AAnPBs compared to total prokaryotes reveal their equal importance in peatlands

Our data revealed that compared to total prokaryotes, prokaryotic oxygenic phototrophs (namely cyanobacteria), chemoautotrophs and AAnPBs were equally abundant. Prokaryotic oxygenic phototrophs and chemoautotrophs represented ~8% and ~10% of total prokaryotes, respectively in Counozouls and ~16% and ~12%, respectively in Männikjärve (Figure A10A,B). These results showed that chemoautotrophs were more or less as abundant as oxygenic phototrophs and possibly equally contributed to CO_2 fixation in peatlands. This contradicts the first estimates of phototrophic and chemoautotrophic CO_2 fixation rates in

peatlands showing that chemoautotrophic CO_2 assimilation represented less than 1% of oxygenic phototrophic CO_2 fixation (Gilbert et al., 1998). It is also important to note that the CBB cycle is not the only pathway for chemoautotrophic CO_2 fixation. Other alternatives include the rTCA cycle, the HP/HB cycle and the reductive acetyl-CoA pathway (Berg, 2011). The importance of these C-fixing pathways has not yet been elucidated in peatlands, and should be investigated shortly to have a full picture of microbial carbon fixation in peatlands. In addition, better resolution of abundance patterns between phototrophs and chemoautotrophs over different spatial and temporal scales could be achieved by RNA quantification. Furthermore, our results show that AAnPBs represented ~8% of total prokaryotes in Counozouls and ~15% of total prokaryotes in Männikjärve (Figure A10), suggesting they may play a significant role in the C cycle of peatlands as some strains possessing CBB cycle genes can actively fix atmospheric CO_2 (Graham et al., 2018; Tang et al., 2021). Altogether these results show that further work is urgently needed to better quantify the contribution of micro-organisms to peatland CO_2 uptake as current estimates based on sole oxygenic phototrophs (Hamard, Céréghino, et al., 2021) may be strongly underestimated. Soils are also facing important climate and land use changes which can profoundly affect soil microbiomes and their functions (IPCC, 2023; Lode et al., 2017; Solomon et al., 2007). Changing soil microbiomes can notably impact C fixation and emissions (Blankinship et al., 2011; Le Geay et al., 2024; Li et al., 2022; Zhou et al., 2020). These changes could lead to enhanced microbial CO_2 fixation in some soils, which could mitigate global changes (Le Geay et al., 2024; Qiu et al., 2020; Strack et al., 2022). Therefore, knowing the contribution of the different CFMs and their metabolic pathway to soil microbial CO_2 fixation is also a key forecast for the changes in the soil C cycle.

To conclude, this study shows that ddPCR can be optimized to amplify targets coming from a complex matrix such as peat and can be used to target both universal markers (16S rRNA gene) and specific markers (e.g., 23S rRNA, *cbbL* or *pufM* genes). Taken together, the results of this study support the effective use of ddPCR to analyse target gene concentrations in different peatland types and at different depths. These results further highlight a complex picture in which major and emerging CFMs may all play a key role in peatland microbial CO_2 fixation. This requires further support in the future to better understand the peatland C cycle. Using a cutting-edge method such as ddPCR can therefore help to better understand the relevance and contribution of CFMs to the soil C cycle. Microbial quantification, which simplifies the quantification of functional genes, provides a better understanding of microbial ecology and its underlying processes within the ecosystem functioning.

AUTHOR CONTRIBUTIONS

Marie Le Geay: Conceptualization; writing – original draft; data curation; formal analysis; methodology; writing – review and editing; funding acquisition. **Kyle Mayers:** Writing – review and editing; methodology; supervision. **Martin Küttim:** Investigation; writing – review and editing. **Béatrice Lauga:** Conceptualization; writing – review and editing; methodology; supervision. **Vincent E. J. Jassey:** Supervision; conceptualization; investigation; writing – review and editing; funding acquisition.

ACKNOWLEDGEMENTS

This work has been supported by the MIXOPEAT (Grant No. ANR-17-CE01-0007 to VEJJ) and BALANCE (Grant No. ANR-23-ERCC-0001-01 to VEJJ) projects funded by the French National Research Agency. This study has been partially supported through the grant EUR TESS (Grant No. ANR-18-EURE-0018 to MLG) in the framework of the Programme des Investissements d'Avenir. We thank the *Plateforme Analyses Physico-Chimiques* from the *Centre de Recherche sur la Biodiversité et l'Environnement* (Université de Toulouse, France).

CONFLICT OF INTEREST STATEMENT

The authors declare that there are no conflicts of interest.

DATA AVAILABILITY STATEMENT

The data that supports the findings of this study can be find in FigShare (10.6084/m9.figshare.25967902).

ORCID

Marie Le Geay https://orcid.org/0009-0007-6098-7942
Béatrice Lauga https://orcid.org/0000-0001-5997-1176
Vincent E. J. Jassey https://orcid.org/0000-0002-1450-2437

REFERENCES

Achenbach, L.A., Carey, J. & Madigan, M.T. (2001) Photosynthetic and phylogenetic primers for detection of anoxygenic phototrophs in natural environments. *Applied and Environmental Microbiology*, 67, 2922–2926. Available from: https://doi.org/10.1128/AEM.67.7.2922-2926.2001

Alfreider, A. & Bogensperger, T. (2018) Specific detection of form IA rubisCO genes in chemoautotrophic bacteria. *Journal of Basic Microbiology*, 58, 712–716. Available from: https://doi.org/10.1002/JOBM.201800136

Bay, S.K., Dong, X., Bradley, J.A., Leung, P.M., Grinter, R., Jirapanjawat, T. et al. (2021) Trace gas oxidizers are widespread and active members of soil microbial communities. *Nature Microbiology*, 2021(6), 246–256. Available from: https://doi.org/10.1038/s41564-020-00811-w

Bengtsson, M.M., Wagner, K., Schwab, C., Urich, T. & Battin, T.J. (2018) Light availability impacts structure and function of phototrophic stream biofilms across domains and trophic levels.

Molecular Ecology, 27, 2913–2925. Available from: https://doi.org/10.1111/MEC.14696

Berg, I.A. (2011) Ecological aspects of the distribution of different autotrophic CO_2 fixation pathways. *Applied and Environmental Microbiology*, 77, 1925–1936. Available from: https://doi.org/10.1128/AEM.02473-10

Blankinship, J.C., Niklaus, P.A. & Hungate, B.A. (2011) A meta-analysis of responses of soil biota to global change. *Oecologia*, 165, 553–565. Available from: https://doi.org/10.1007/S00442-011-1909-0/TABLES/3

Boschker, H.T.S., Vasquez-Cardenas, D., Bolhuis, H., Moerdijk-Poortvliet, T.W.C. & Moodley, L. (2014) Chemoautotrophic carbon fixation rates and active bacterial communities in intertidal marine sediments. *PLoS ONE*, 9, e101443. Available from: https://doi.org/10.1371/JOURNAL.PONE.0101443

Bressan, M., Trinsoutrot Gattin, I., Desaire, S., Castel, L., Gangneux, C. & Laval, K. (2015) A rapid flow cytometry method to assess bacterial abundance in agricultural soil. *Applied Soil Ecology*, 88, 60–68. Available from: https://doi.org/10.1016/J.APSOIL.2014.12.007

Buttler, A., Robroek, B.J.M., Laggoun-Défarge, F., Jassey, V.E.J., Pochelon, C., Bernard, G. et al. (2015) Experimental warming interacts with soil moisture to discriminate plant responses in an ombrotrophic peatland. *Journal of Vegetation Science*, 26, 964–974. Available from: https://doi.org/10.1111/JVS.12296

Béjà, O., Suzuki, M.T., Heidelberg, J.F., Nelson, W.C., Preston, C.M., Hamada, T. et al. (2002) Unsuspected diversity among marine aerobic anoxygenic phototrophs. *Nature*, 415, 630–633. Available from: https://doi.org/10.1038/415630A

Carey, C.C., Ibelings, B.W., Hoffmann, E.P., Hamilton, D.P. & Brookes, J.D. (2012) Eco-physiological adaptations that favour freshwater cyanobacteria in a changing climate. *Water Research*, 46, 1394–1407. Available from: https://doi.org/10.1016/J.WATRES.2011.12.016

Delarue, F., Laggoun-Défarge, F., Disnar, J.R., Lottier, N. & Gogo, S. (2011) Organic matter sources and decay assessment in a sphagnum-dominated peatland (Le Forbonnet, Jura Mountains, France): impact of moisture conditions. *Biogeochemistry*, 106, 39–52. Available from: https://doi.org/10.1007/S10533-010-9410-0/FIGURES/5

Demeke, T., Eng, M., Holigroski, M. & Lee, S.J. (2021) Effect of amount of DNA on digital PCR assessment of genetically engineered canola and soybean events. *Food Analytical Methods*, 14, 372–379. Available from: https://doi.org/10.1007/S12161-020-01889-Y/TABLES/4

Djemiel, C., Plassard, D., Terrat, S., Crouzet, O., Sauze, J., Mondy, S. et al. (2020) µgreen-db: a reference database for the 23S rRNA gene of eukaryotic plastids and cyanobacteria. *Scientific Reports*, 10, 5915. Available from: https://doi.org/10.1038/S41598-020-62555-1

Du, H., Jiao, N., Hu, Y. & Zeng, Y. (2006) Real-time PCR for quantification of aerobic anoxygenic phototrophic bacteria based on pufM gene in marine environment. *Journal of Experimental Marine Biology and Ecology*, 329, 113–121. Available from: https://doi.org/10.1016/J.JEMBE.2005.08.009

Feng, Y., Lin, X., Mao, T. & Zhu, J. (2011) Diversity of aerobic anoxygenic phototrophic bacteria in paddy soil and their response to elevated atmospheric CO_2. *Microbial Biotechnology*, 4, 74–81. Available from: https://doi.org/10.1111/J.1751-7915.2010.00211.X

Figueroa, I.A., Barnum, T.P., Somasekhar, P.Y., Carlström, C.I., Engelbrektson, A.L. & Coates, J.D. (2018) Metagenomics-guided analysis of microbial chemolithoautotrophic phosphite oxidation yields evidence of a seventh natural CO_2 fixation pathway. *Proceedings of the National Academy of Sciences of the United States of America*, 115, E92–E101. Available from: https://doi.org/10.1073/PNAS.1715549114/SUPPL_FILE/PNAS.201715549SI.PDF

Frossard, A., Hammes, F. & Gessner, M.O. (2016) Flow cytometric assessment of bacterial abundance in soils, sediments and sludge. *Frontiers in Microbiology*, 7, 195298. Available from: https://doi.org/10.3389/FMICB.2016.00903/BIBTEX

Frostegård, A. & Bååth, E. (1996) The use of phospholipid fatty acid analysis to estimate bacterial and fungal biomass in soil. *Biology and Fertility of Soils*, 22, 59–65. Available from: https://doi.org/10.1007/BF00384433

Ge, T., Wu, X., Chen, X., Yuan, H., Zou, Z., Li, B. et al. (2013) Microbial phototrophic fixation of atmospheric CO_2 in China subtropical upland and paddy soils. *Geochimica et Cosmochimica Acta*, 113, 70–78. Available from: https://doi.org/10.1016/J.GCA.2013.03.020

Gilbert, D., Amblard, C., Bourdier, G. & Francez, A. (1998) The microbial loop at the surface of a peatland:structure, function, and impact of nutrient input. *Microbial Ecology*, 35, 83–93. Available from: https://doi.org/10.1007/s002489900062

Gomez-Saez, G.V., Ristova, P.P., Sievert, S.M., Elvert, M., Hinrichs, K.U. & Bühring, S.I. (2017) Relative importance of chemoautotrophy for primary production in a light exposed marine shallow hydrothermal system. *Frontiers in Microbiology*, 8, 257720. Available from: https://doi.org/10.3389/FMICB.2017.00702/BIBTEX

Graham, E.D., Heidelberg, J.F. & Tully, B.J. (2018) Potential for primary productivity in a globally-distributed bacterial phototroph. *The ISME Journal*, 12, 1861–1866. Available from: https://doi.org/10.1038/S41396-018-0091-3

Guo, G., Kong, W., Liu, J., Zhao, J., Du, H., Zhang, X. et al. (2015) Diversity and distribution of autotrophic microbial community along environmental gradients in grassland soils on the Tibetan plateau. *Applied Microbiology and Biotechnology*, 99, 8765–8776. Available from: https://doi.org/10.1007/S00253-015-6723-X

Hamard, S., Céréghino, R., Barret, M., Sytiuk, A., Lara, E., Dorrepaal, E. et al. (2021) Contribution of microbial photosynthesis to peatland carbon uptake along a latitudinal gradient. *Journal of Ecology*, 109, 3424–3441. Available from: https://doi.org/10.1111/1365-2745.13732

Hamard, S., Küttim, M., Céréghino, R. & Jassey, V.E.J. (2021) Peatland microhabitat heterogeneity drives phototrophic microbe distribution and photosynthetic activity. *Environmental Microbiology*, 23, 6811–6827. Available from: https://doi.org/10.1111/1462-2920.15779

Hammes, F., Goldschmidt, F., Vital, M., Wang, Y. & Egli, T. (2010) Measurement and interpretation of microbial adenosine triphosphate (ATP) in aquatic environments. *Water Research*, 44, 3915–3923. Available from: https://doi.org/10.1016/J.WATRES.2010.04.015

Higuchi, R., Fockler, C., Dollinger, G. & Watson, R. (1993) Kinetic PCR analysis: real-time monitoring of DNA amplification reactions. *Bio/Technology*, 11, 1026–1030. Available from: https://doi.org/10.1038/NBT0993-1026

Hindson, B.J., Ness, K.D., Masquelier, D.A., Belgrader, P., Heredia, N.J., Makarewicz, A.J. et al. (2011) High-throughput droplet digital PCR system for absolute quantitation of DNA copy number. *Analytical Chemistry*, 83, 8604–8610. Available from: https://doi.org/10.1021/AC202028G/SUPPL_FILE/AC202028G_SI_001.PDF

Hou, Y., Chen, S., Zheng, Y., Zheng, X. & Lin, J.M. (2023) Droplet-based digital PCR (ddPCR) and its applications. *TrAC Trends in Analytical Chemistry*, 158, 116897. Available from: https://doi.org/10.1016/J.TRAC.2022.116897

Huang, Q., Huang, Y., Wang, B., Dippold, M.A., Li, H., Li, N. et al. (2022) Metabolic pathways of CO_2 fixing microorganisms determined C-fixation rates in grassland soils along the precipitation gradient. *Soil Biology and Biochemistry*, 172, 108764. Available from: https://doi.org/10.1016/J.SOILBIO.2022.108764

Hügler, M. & Sievert, S.M. (2011) Beyond the Calvin cycle: autotrophic carbon fixation in the ocean. *Annual Review of Marine Science*, 3, 261–289. Available from: https://doi.org/10.1146/ANNUREV-MARINE-120709-142712

IPCC. (2023) In: Core Writing Team, Lee, H. & Romero, J. (Eds.) *Climate change 2023: synthesis report. Contribution of working groups I, II and III to the sixth assessment report of the intergovernmental panel on climate change*. IPCC, AR6 Synthesis Report, 184. Available from: https://doi.org/10.59327/IPCC/AR6-9789291691647

Jassey, V.E.J., Hamard, S., Lepère, C., Céréghino, R., Corbara, B., Küttim, M. et al. (2022) Photosynthetic microorganisms effectively contribute to bryophyte CO_2 fixation in boreal and tropical regions. *ISME Communications*, 2022(2), 1–10. Available from: https://doi.org/10.1038/s43705-022-00149-w

Jassey, V.E.J., Signarbieux, C., Hättenschwiler, S., Bragazza, L., Buttler, A., Delarue, F. et al. (2015) An unexpected role for mixotrophs in the response of peatland carbon cycling to climate warming. *Scientific Reports*, 5, 1–10. Available from: https://doi.org/10.1038/srep16931

Karl, D.M. (1980) Cellular nucleotide measurements and applications in microbial ecology. *Microbiological Reviews*, 44, 739–796. Available from: https://doi.org/10.1128/MR.44.4.739-796.1980

Keselman, H.J. & Rogan, J.C. (1977) The Tukey multiple comparison test: 1953-1976. *Psychological Bulletin*, 84, 1050–1056. Available from: https://doi.org/10.1037/0033-2909.84.5.1050

Keshri, J., Yousuf, B., Mishra, A. & Jha, B. (2015) The abundance of functional genes, cbbL, nifH, amoA and apsA, and bacterial community structure of intertidal soil from Arabian Sea. *Microbiological Research*, 175, 57–66. Available from: https://doi.org/10.1016/J.MICRES.2015.02.007

Koblížek, M., Béjà, O., Bidigare, R.R., Christensen, S., Benitez-Nelson, B., Vetriani, C. et al. (2003) Isolation and characterization of Erythrobacter sp. strains from the upper ocean. *Archives of Microbiology*, 180, 327–338. Available from: https://doi.org/10.1007/S00203-003-0596-6

Kokkoris, V., Vukicevich, E., Richards, A., Thomsen, C. & Hart, M.M. (2021) Challenges using droplet digital PCR for environmental samples. *Applied Microbiology*, 1, 74–88. Available from: https://doi.org/10.3390/APPLMICROBIOL1010007

Kusian, B. & Bowien, B. (1997) Organization and regulation of cbb CO_2 assimilation genes in autotrophic bacteria. *FEMS Microbiology Reviews*, 21, 135–155. Available from: https://doi.org/10.1111/J.1574-6976.1997.TB00348.X

Le Geay, M., Lauga, B., Walcker, R. & Jassey, V.E.J. (2024) A meta-analysis of peatland microbial diversity and function responses to climate change. *Soil Biology and Biochemistry*, 189, 109287. Available from: https://doi.org/10.1016/J.SOILBIO.2023.109287

Lew, S., Lew, M. & Koblížek, M. (2016) Influence of selected environmental factors on the abundance of aerobic anoxygenic phototrophs in peat-bog lakes. *Environmental Science and Pollution Research*, 23, 13853–13863. Available from: https://doi.org/10.1007/S11356-016-6521-8/TABLES/4

Li, Y., Ma, J., Yu, Y., Li, Y., Shen, X., Huo, S. et al. (2022) Effects of multiple global change factors on soil microbial richness, diversity and functional gene abundances: a meta-analysis. *Science of the Total Environment*, 815, 152737. Available from: https://doi.org/10.1016/J.SCITOTENV.2021.152737

Liao, H., Hao, X., Qin, F., Delgado-Baquerizo, M., Liu, Y., Zhou, J. et al. (2023) Microbial autotrophy explains large-scale soil CO_2 fixation. *Global Change Biology*, 29, 231–242. Available from: https://doi.org/10.1111/GCB.16452

Lin, X., Green, S., Tfaily, M.M., Prakash, O., Konstantinidis, K.T., Corbett, J.E. et al. (2012) Microbial community structure and activity linked to contrasting biogeochemical gradients in bog and fen environments of the glacial Lake Agassiz peatland. *Applied and Environmental Microbiology*, 78, 7023–7031. Available from: https://doi.org/10.1128/AEM.01750-12

Liu, Z., Sun, Y., Zhang, Y., Feng, W., Lai, Z., Fa, K. et al. (2018) Metagenomic and 13C tracing evidence for autotrophic atmospheric carbon absorption in a semiarid desert. *Soil Biology and Biochemistry*, 125, 156–166. Available from: https://doi.org/10.1016/J.SOILBIO.2018.07.012

Lode, E., Küttim, M. & Kiivit, I.K. (2017) Indicative effects of climate change on groundwater levels in estonian raised bogs over 50 years. *Mires and Peat*, 19, 15, 1–21. Available from: https://doi.org/10.19189/MAP.2016.OMB.255

Mpamah, P.A., Taipale, S., Rissanen, A.J., Biasi, C. & Nykänen, H.K. (2017) The impact of long-term water level draw-down on microbial biomass: a comparative study from two peatland sites with different nutrient status. *European Journal of Soil Biology*, 80, 59–68. Available from: https://doi.org/10.1016/J.EJSOBI.2017.04.005

Mullis, K., Faloona, F., Scharf, S., Saiki, R., Horn, G. & Erlich, H. (1986) Specific enzymatic amplification of DNA in vitro: the polymerase chain reaction. *Cold Spring Harbor Symposia on Quantitative Biology*, 51, 263–273. Available from: https://doi.org/10.1101/SQB.1986.051.01.032

Nakagawa, S. & Takai, K. (2008) Deep-sea vent chemoautotrophs: diversity, biochemistry and ecological significance. *FEMS Microbiology Ecology*, 65, 1–14. Available from: https://doi.org/10.1111/J.1574-6941.2008.00502.X

Nichols, J.E. & Peteet, D.M. (2019) Rapid expansion of northern peatlands and doubled estimate of carbon storage. *Nature Geoscience*, 12, 917–921. Available from: https://doi.org/10.1038/s41561-019-0454-z

Nowak, M.E., Beulig, F., Von Fischer, J., Muhr, J., Küsel, K. & Trumbore, S.E. (2015) Autotrophic fixation of geogenic CO_2 by microorganisms contributes to soil organic matter formation and alters isotope signatures in a wetland mofette. *Biogeosciences*, 12, 7169–7183. Available from: https://doi.org/10.5194/BG-12-7169-2015

Pearman, J.K., Biessy, L., Howarth, J.D., Vandergoes, M.J., Rees, A. & Wood, S.A. (2022) Deciphering the molecular signal from past and alive bacterial communities in aquatic sedimentary archives. *Molecular Ecology Resources*, 22, 877–890. Available from: https://doi.org/10.1111/1755-0998.13515

Pinheiro, L.B., Coleman, V.A., Hindson, C.M., Herrmann, J., Hindson, B.J., Bhat, S. et al. (2012) Evaluation of a droplet digital polymerase chain reaction format for DNA copy number quantification. *Analytical Chemistry*, 84, 1003–1011. Available from: https://doi.org/10.1021/AC202578X/SUPPL_FILE/AC202578X_SI_002.PDF

Qiu, C., Zhu, D., Ciais, P., Guenet, B. & Peng, S. (2020) The role of northern peatlands in the global carbon cycle for the 21st century. *Global Ecology and Biogeography*, 29, 956–973. Available from: https://doi.org/10.1111/GEB.13081

Quast, C., Pruesse, E., Yilmaz, P., Gerken, J., Schweer, T., Yarza, P. et al. (2013) The SILVA ribosomal RNA gene database project: improved data processing and web-based tools. *Nucleic Acids Research*, 41, D590–D596. Available from: https://doi.org/10.1093/NAR/GKS1219

Reczuga, M.K., Lamentowicz, M., Mulot, M., Mitchell, E.A.D., Buttler, A., Chojnicki, B. et al. (2018) Predator–prey mass ratio drives microbial activity under dry conditions in sphagnum peatlands. *Ecology and Evolution*, 8, 5752–5764. Available from: https://doi.org/10.1002/ECE3.4114

Rodríguez, A., Rodríguez, M., Córdoba, J.J. & Andrade, M.J. (2015) Design of primers and probes for quantitative real-time PCR methods. *Methods in Molecular Biology*, 1275, 31–56. Available from: https://doi.org/10.1007/978-1-4939-2365-6_3/COVER

Rowlands, V., Rutkowski, A.J., Meuser, E., Carr, T.H., Harrington, E.A. & Barrett, J.C. (2019) Optimisation of robust singleplex and multiplex droplet digital PCR assays for high confidence mutation detection in circulating tumour DNA. *Scientific*

Reports, 9, 12620. Available from: https://doi.org/10.1038/S41598-019-49043-X

RStudio Team. (2020) RStudio: integrated development for R.

Sato-Takabe, Y., Hirose, S., Hori, T. & Hanada, S. (2020) Abundance and spatial distribution of aerobic anoxygenic phototrophic bacteria in Tama River, Japan. *Water*, 12, 150. Available from: https://doi.org/10.3390/W12010150

Sato-Takabe, Y., Nakao, H., Kataoka, T., Yokokawa, T., Hamasaki, K., Ohta, K. et al. (2016) Abundance of common aerobic anoxygenic phototrophic bacteria in a coastal aquaculture area. *Frontiers in Microbiology*, 7, 1996. Available from: https://doi.org/10.3389/FMICB.2016.01996

Selesi, D., Pattis, I., Schmid, M., Kandeler, E. & Hartmann, A. (2007) Quantification of bacterial RubisCO genes in soils by cbbL targeted real-time PCR. *Journal of Microbiological Methods*, 69, 497–503. Available from: https://doi.org/10.1016/J.MIMET.2007.03.002

Shapiro, S.S. & Wilk, M.B. (1965) An analysis of variance test for normality (complete samples). *Biometrika*, 52, 591–611. Available from: https://doi.org/10.1093/BIOMET/52.3-4.591

Sherwood, A.R. & Presting, G.G. (2007) Universal primers amplify a 23S rDNA plastid marker in eukaryotic algae and cyanobacteria. *Journal of Phycology*, 43, 605–608. Available from: https://doi.org/10.1111/J.1529-8817.2007.00341.X

Shively, J.M., Van Keulen, G. & Meijer, W.G. (1998) Something from almost nothing: carbon dioxide fixation in chemoautotrophs. *Annual Review of Microbiology*, 52, 191–230. Available from: https://doi.org/10.1146/ANNUREV.MICRO.52.1.191

Sidstedt, M., Jansson, L., Nilsson, E., Noppa, L., Forsman, M., Rådström, P. et al. (2015) Humic substances cause fluorescence inhibition in real-time polymerase chain reaction. *Analytical Biochemistry*, 487, 30–37. Available from: https://doi.org/10.1016/J.AB.2015.07.002

Solomon, S., Qin, D., Manning, M., Chen, Z., Marquis, M., Averyt, K.B. et al. (2007) *Contribution of working group I to the fourth assessment report of the intergovernmental panel on climate change, 2007*. Cambridge University Press. Available from: https://archive.ipcc.ch/publications_and_data/publications_ipcc_fourth_assessment_report_wg1_report_the_physical_science_basis.htm [Accessed 5th June 2024].

Strack, M., Davidson, S.J., Hirano, T. & Dunn, C. (2022) The potential of peatlands as nature-based climate solutions. *Current Climate Change Reports*, 8, 71–82. Available from: https://doi.org/10.1007/s40641-022-00183-9

Sytiuk, A., Céréghino, R., Hamard, S., Delarue, F., Dorrepaal, E., Küttim, M. et al. (2022). Biochemical traits enhance the trait concept in Sphagnum ecology. *Oikos*, 4, e09119. Available from: https://doi.org/10.1111/OIK.09119

Sytiuk, A., Céréghino, R., Hamard, S., Delarue, F., Guittet, A., Barel, J.M. et al. (2022) Predicting the structure and functions of peatland microbial communities from sphagnum phylogeny, anatomical and morphological traits and metabolites. *Journal of Ecology*, 110, 80–96. Available from: https://doi.org/10.1111/1365-2745.13728

Sánchez-Andrea, I., Guedes, I. A., Hornung, B., Boeren, S., Lawson, C. E., Sousa, D. Z. et al. (2020). The reductive glycine pathway allows autotrophic growth of Desulfovibrio desulfuricans. *Nature Communications,* 11, 1–12. Available from: https://doi.org/10.1038/s41467-020-18906-7

Tang, K., Jia, L., Yuan, B., Yang, S., Li, H., Meng, J. et al. (2018) Aerobic anoxygenic phototrophic bacteria promote the development of biological soil crusts. *Frontiers in Microbiology*, 9, 2715. Available from: https://doi.org/10.3389/FMICB.2018.02715

Tang, K., Liu, Y., Zeng, Y., Feng, F., Jin, K. & Yuan, B. (2021) An aerobic anoxygenic phototrophic bacterium fixes CO_2 via the Calvin–Benson–Bassham cycle. *BioRxiv*, 2021(4), 29.441244. Available from: https://doi.org/10.1101/2021.04.29.441244

Taylor, S.C., Laperriere, G. & Germain, H. (2017) Droplet digital PCR versus qPCR for gene expression analysis with low abundant targets: from variable nonsense to publication quality data. *Scientific Reports*, 7, 1–8. Available from: https://doi.org/10.1038/s41598-017-02217-x

Vogelstein, B. & Kinzler, K.W. (1999) Digital PCR. *Proceedings of the National Academy of Sciences of the United States of America*, 96, 9236–9241. Available from: https://doi.org/10.1073/PNAS.96.16.9236

Wang, D., Wang, S., Du, X., He, Q., Liu, Y., Wang, Z. et al. (2022) ddPCR surpasses classical qPCR technology in quantitating bacteria and fungi in the environment. *Molecular Ecology Resources*, 22, 2587–2598. Available from: https://doi.org/10.1111/1755-0998.13644

Wang, X., Howe, S., Deng, F. & Zhao, J. (2021) Current applications of absolute bacterial quantification in microbiome studies and decision-making regarding different biological questions. *Microorganisms*, 9, 1797. Available from: https://doi.org/10.3390/MICROORGANISMS9091797

Wang, X., Li, W., Xiao, Y., Cheng, A., Shen, T., Zhu, M. et al. (2021) Abundance and diversity of carbon-fixing bacterial communities in karst wetland soil ecosystems. *Catena*, 204, 105418. Available from: https://doi.org/10.1016/J.CATENA.2021.105418

Wang, Y., Huang, Y., Zeng, Q., Liu, D. & An, S. (2023) Biogeographic distribution of autotrophic bacteria was more affected by precipitation than by soil properties in an arid area. *Frontiers in Microbiology*, 14, 1303469. Available from: https://doi.org/10.3389/FMICB.2023.1303469/BIBTEX

Wen, X., Unger, V., Jurasinski, G., Koebsch, F., Horn, F., Rehder, G. et al. (2018) Predominance of methanogens over methanotrophs in rewetted fens characterized by high methane emissions. *Biogeosciences*, 15, 6519–6536. Available from: https://doi.org/10.5194/BG-15-6519-2018

Wickham, H. (2016) ggpolt2 Elegant Graphics for Data Analysis 211.

Witte, A.K., Mester, P., Fister, S., Witte, M., Schoder, D. & Rossmanith, P. (2016) A systematic investigation of parameters influencing droplet rain in the listeria monocytogenes prfA assay - reduction of ambiguous results in ddPCR. *PLoS ONE*, 11, e0168179. Available from: https://doi.org/10.1371/JOURNAL.PONE.0168179

Xiao, K.Q., Bao, P., Bao, Q.L., Jia, Y., Huang, F.Y., Su, J.Q. et al. (2014) Quantitative analyses of ribulose-1,5-bisphosphate carboxylase/oxygenase (RubisCO) large-subunit genes (cbbL) in typical paddy soils. *FEMS Microbiology Ecology*, 87, 89–101. Available from: https://doi.org/10.1111/1574-6941.12193

Xu, X., Thornton, P.E. & Post, W.M. (2013) A global analysis of soil microbial biomass carbon, nitrogen and phosphorus in terrestrial ecosystems. *Global Ecology and Biogeography*, 22, 737–749. Available from: https://doi.org/10.1111/GEB.12029

Xu, Z., Wang, S., Wang, Z., Dong, Y., Zhang, Y., Liu, S. et al. (2021) Effect of drainage on microbial enzyme activities and communities dependent on depth in peatland soil. *Biogeochemistry*, 155, 323–341. Available from: https://doi.org/10.1007/S10533-021-00828-1/FIGURES/7

Xue, J., Caton, K. & Sherchan, S.P. (2018) Comparison of next-generation droplet digital PCR with quantitative PCR for enumeration of Naegleria fowleri in environmental water and clinical samples. *Letters in Applied Microbiology*, 67, 322–328. Available from: https://doi.org/10.1111/LAM.13051

Yang, J., Kang, Y., Sakurai, K. & Ohnishi, K. (2017) Fixation of carbon dioxide by chemoautotrophic bacteria in grassland soil under dark conditions. Acta Agriculturae Scandinavica, section B—Soil & Plant. *Science*, 67, 362–371. Available from: https://doi.org/10.1080/09064710.2017.1281433

Yin, T., Qin, H.L., Yan, C.R., Liu, Q. & He, W.Q. (2022) Low soil carbon saturation deficit limits the abundance of cbbL-carrying bacteria under long-term no-tillage maize cultivation in northern

China. *Journal of Integrative Agriculture*, 21, 2399–2412. Available from: https://doi.org/10.1016/S2095-3119(21)63800-5

Yuan, H., Ge, T., Chen, C., O'Donnell, A.G. & Wu, J. (2012) Significant role for microbial autotrophy in the sequestration of soil carbon. *Applied and Environmental Microbiology*, 78, 2328–2336. Available from: https://doi.org/10.1128/AEM.06881-11

Zhao, K., Zhang, B., Li, J., Li, B. & Wu, Z. (2021) The autotrophic community across developmental stages of biocrusts in the Gurbantunggut Desert. *Geoderma*, 388, 114927. Available from: https://doi.org/10.1016/J.GEODERMA.2021.114927

Zhao, Y., Xia, Q., Yin, Y. & Wang, Z. (2016) Comparison of droplet digital PCR and quantitative PCR assays for quantitative detection of *Xanthomonas citri* Subsp. citri. *PLoS ONE*, 11, e0159004. Available from: https://doi.org/10.1371/JOURNAL.PONE.0159004

Zhou, Z., Wang, C. & Luo, Y. (2020) Meta-analysis of the impacts of global change factors on soil microbial diversity and functionality. *Nature Communications*, 11, 1–10. Available from: https://doi.org/10.1038/s41467-020-16881-7

Øvreås, L., Forney, L., Daae, F.L. & Torsvik, V. (1997) Distribution of bacterioplankton in meromictic Lake Saelenvannet, as determined by denaturing gradient gel electrophoresis of PCR-amplified gene fragments coding for 16S rRNA. *Applied and Environmental Microbiology*, 63, 3367–3373. Available from: https://doi.org/10.1128/AEM.63.9.3367-3373.1997

How to cite this article: Le Geay, M., Mayers, K., Küttim, M., Lauga, B. & Jassey, V.E.J. (2024) Development of a digital droplet PCR approach for the quantification of soil micro-organisms involved in atmospheric CO_2 fixation. *Environmental Microbiology*, 26(6), e16666. Available from: https://doi.org/10.1111/1462-2920.16666

APPENDIX A

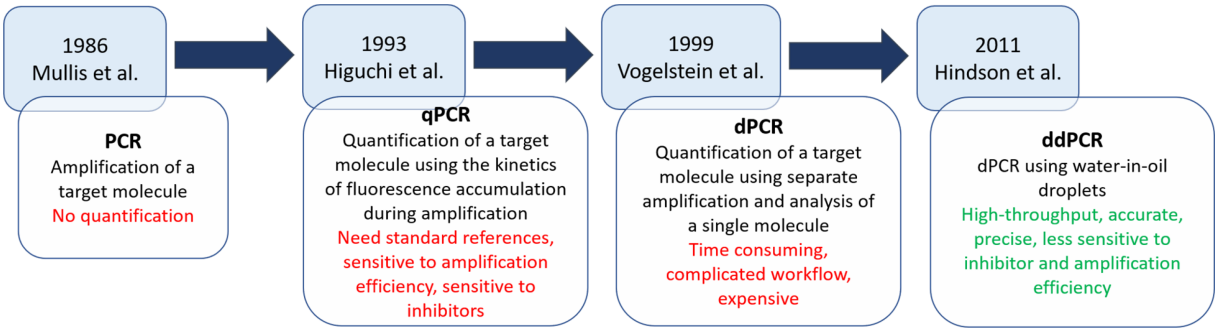

FIGURE A1 Different molecular methods to quantify DNA (inspired from Hou et al., 2023). dPCR, digital polymerase chain reaction; ddPCR, digital droplet polymerase chain reaction; PCR, polymerase chain reaction; qPCR, real-time polymerase chain reaction.

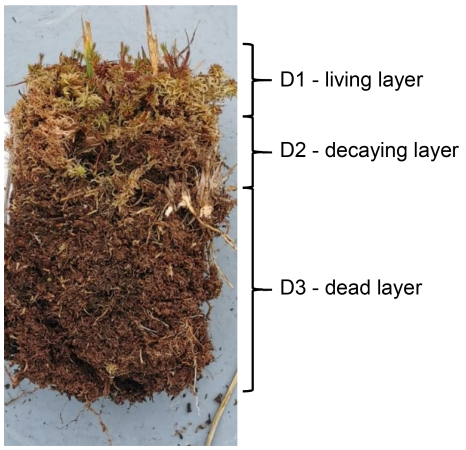

FIGURE A2 Sphagnum shoots highlighting the living layer (green capitulum part), the decaying layer (dying part of Sphagnum that is yellowish) and the dead layer (where Sphagnum dies and starts to decompose that is brownish).

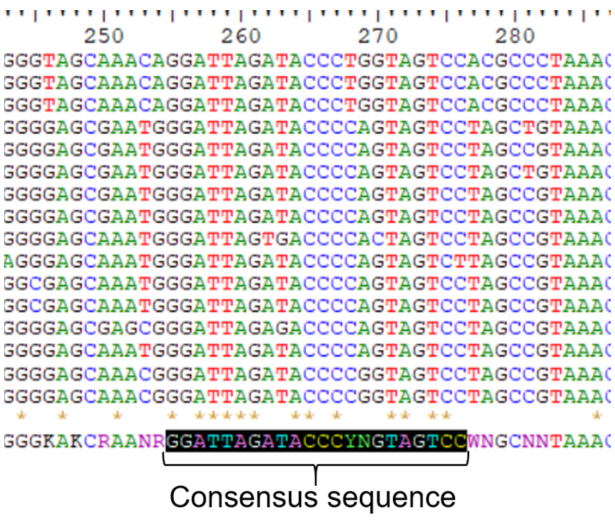

FIGURE A3 Aligned sequence and consensus sequence for the design of the 23S255f forward primer to target the 23S rRNA gene with digital droplet polymerase chain reaction.

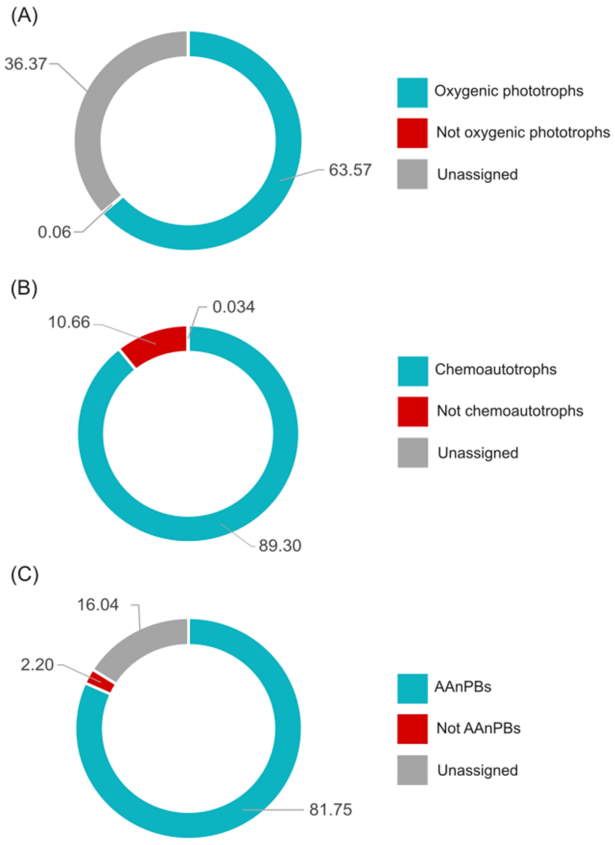

FIGURE A4 Specificity and coverage of primers used in this study to target (A) oxygenic phototrophs, (B) chemoautotrophs and (C) aerobic anoxygenic phototrophic bacteria (AAnPBs). Each doughnut plot represents the mean of bacterial groups belonging to the targeted group (either oxygenic phototrophs, chemoautotrophs or AAnPBs) along with unassigned and untargeted bacterial groups.

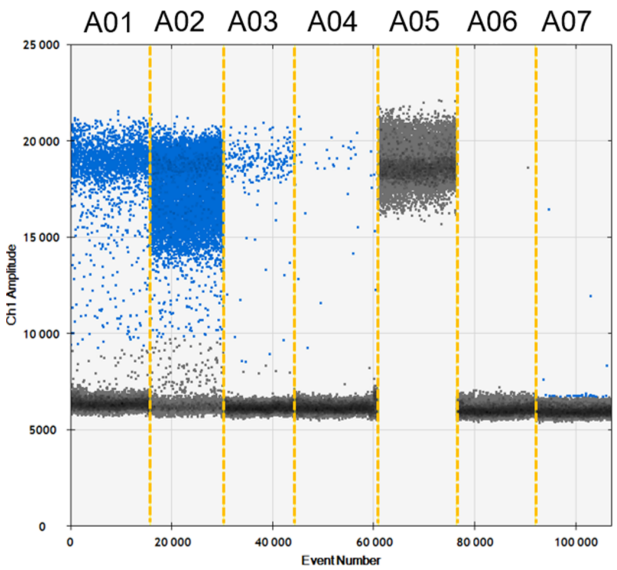

FIGURE A5 Results of digital droplet polymerase chain reaction assays for the *16S rRNA* gene targeting prokaryotes. Only samples from the living layer (D1; 0–5 cm) from Counozouls were used for *16S rRNA* gene assays. A01 = DNA template diluted 10 times, A02 = DNA template not diluted, A03 = DNA template diluted 100 times, A04 = DNA template diluted 1,000 times, A05 = *E. coli* DNA (positive control), A06 and A07 = ultrapure water (negative controls).

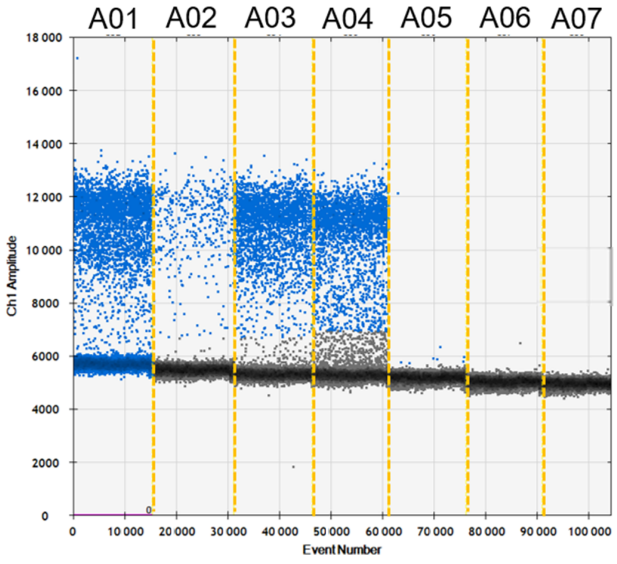

FIGURE A6 Results of digital droplet polymerase chain reaction assays for the *23S rRNA* gene targeting oxygenic phototrophs. Samples from the living layer (D1; 0–5 cm), the decaying layer (D2; 5–10 cm) and the dead layer (D3; 10–15 cm) from Counozouls were used for *23S rRNA* gene assays. A01 = D1, DNA template diluted 10 times, A02 = D1, DNA template diluted 100 times, A03 = D2, DNA template diluted 10 times, A04 = D3, DNA template diluted 10 times, A05 = *E. coli* DNA (negative control), A06 and A07 = ultrapure water (negative controls).

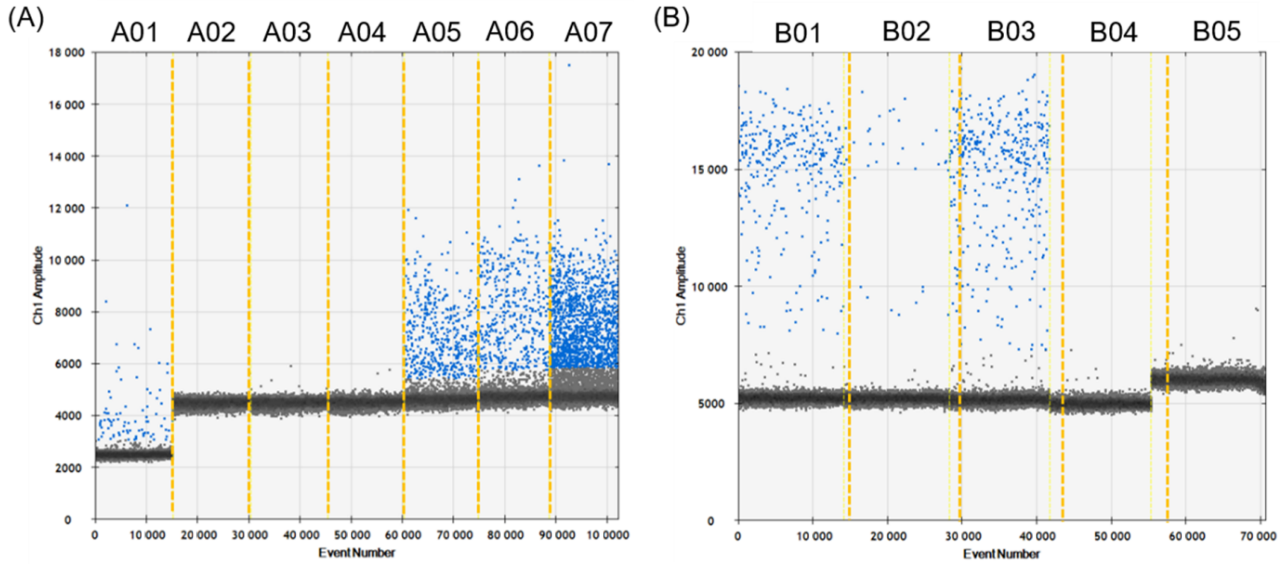

FIGURE A7 Results of digital droplet polymerase chain reaction (ddPCR) assays for the *cbbL* gene targeting chemoautotrophs before (A) and after (B) optimization of ddPCR parameters. Samples from the living layer (D1; 0–5 cm), the decaying layer (D2; 5–10 cm) and the dead layer (D3; 10–15 cm) from Counozouls were used for *cbbL* gene assays. Before ddPCR parameters optimization: A01 = D1, DNA template diluted 10 times, A02 and A03 = ultrapure water (negative controls), A04 = *E. coli* DNA (negative control), A05 = D3, DNA template diluted 10 times, A06 = D2, DNA template diluted 10 times and A07 = D1, DNA template not diluted. After ddPCR parameters optimization: B01 = D2, DNA template diluted 100 times, B02 = D2, DNA template diluted 1000 times, B03 = D3, DNA template diluted 100 times, B04 = *E. coli* DNA (negative control) and B05 = ultrapure water (negative control).

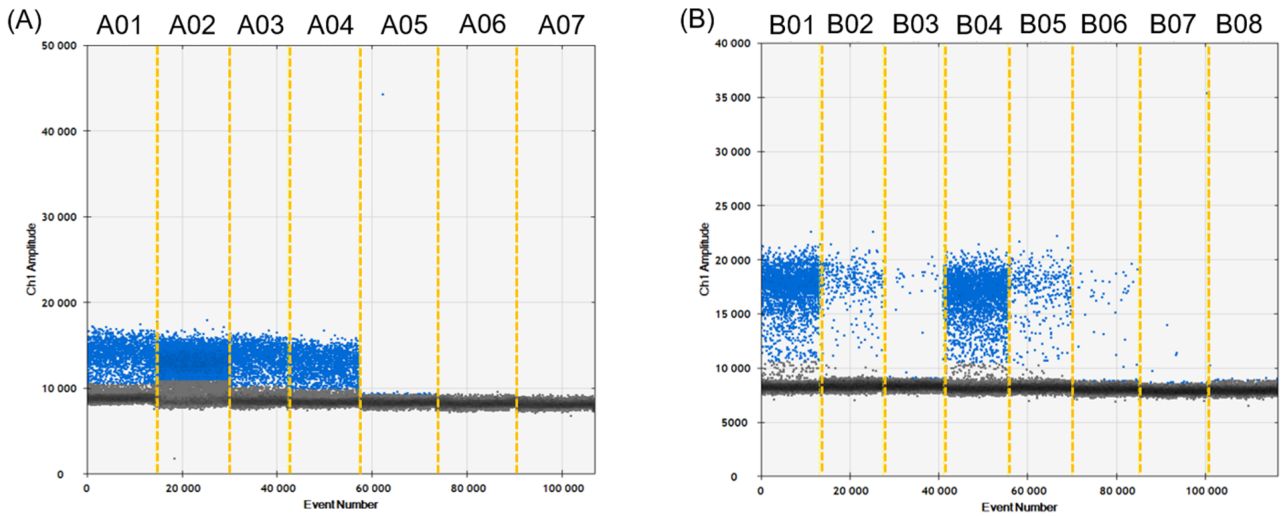

FIGURE A8 Results of digital droplet polymerase chain reaction (ddPCR) assays for the *pufM* gene targeting aerobic anoxygenic phototrophic bacteria before (A) and after (B) optimization of ddPCR parameters. Samples from the living layer (D1; 0–5 cm), the decaying layer (D2; 5–10 cm) and the dead layer (D3; 10–15 cm) from Counozouls were used for *pufM* gene assays. Before ddPCR parameters optimization: A01 = D1, DNA template diluted 10 times, A02 = D1, DNA template not diluted, A03 = D2, DNA template diluted 10 times, A04 = D3, DNA template diluted 10 times, A05 = *E. coli* DNA (negative control), A06 and A07 = ultrapure water (negative controls). After ddPCR parameters optimization: B01 = D2, DNA template diluted 10 times, B02 = D2, DNA template diluted 100 times, B03 = D2, DNA template diluted 1000 times, B04 = D3, DNA template diluted 10 times, B05 = D3, DNA template diluted 100 times, B06 = D3, DNA template diluted 1000 times, B07 = *E. coli* DNA (negative control) and B08 = ultrapure water (negative control).

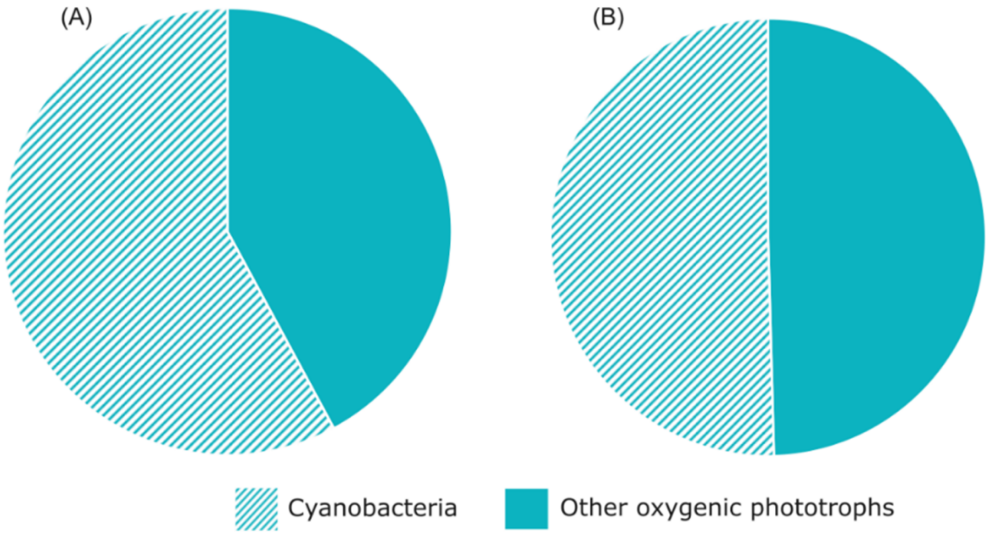

FIGURE A9 Proportion of cyanobacteria among oxygenic phototrophs in Counozouls (A) and Männikjärve (B). Cyanobacteria amount among oxygenic phototrophs was evaluated using sequencing data (data not shown).

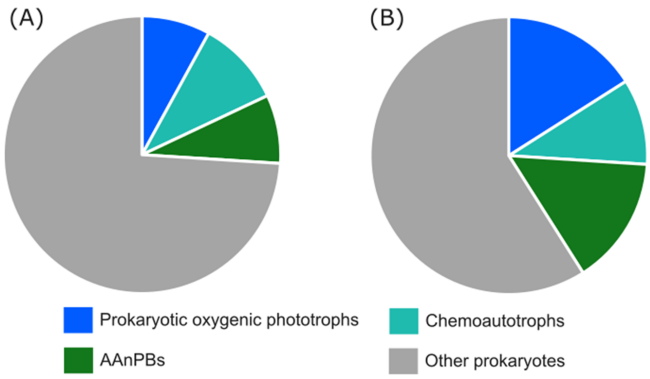

FIGURE A10 Ratios of 23S rRNA gene targeting prokaryotic oxygenic phototrophs, *cbbL* targeting chemoautotrophs and *pufM* targeting aerobic anoxygenic phototrophic bacterias (AAnPBs) in (A) Counozouls (fen) and (B) Männikjärve (bog). In Counozouls, prokaryotic oxygenic phototrophs represented ∼8% of total prokaryotes, chemoautotrophs represented ∼10% of total prokaryotes and AAnPBs represented ∼8% of total prokaryotes. In Männikjärve, prokaryotic oxygenic phototrophs represented ∼16% of total prokaryotes, chemoautotrophs represented ∼12% of total prokaryotes and AAnPBs represented ∼15% of total prokaryotes. Part of prokaryotic oxygenic phototrophs was done using sequencing data (Figure A9).

TABLE A1 Environmental parameters measured in Counozouls and Männikjärve.

ID	Site	Plot	JJA temp	JJA prec	DTN	DOC	VP cover	pH
C01	Counozouls	1	15.2	37	1.718	115.7	44.04762	5.65
C02	Counozouls	2	15.2	37	1.772	99.59	38.9881	5.78
C03	Counozouls	3	15.2	37	1.793	72.57	45.83333	5.9
C04	Counozouls	4	15.2	37	1.818	64.21	60.71429	5.72
C05	Counozouls	5	15.2	37	1.742	66.68	61.30952	5.95
M01	Männikjärve	1	15.8	69	2.0172	51.6	15.77381	5.03
M02	Männikjärve	2	15.8	69	1.358	42.28	16.36905	4.55
M03	Männikjärve	3	15.8	69	1.415	45.94	16.66667	5.4
M04	Männikjärve	4	15.8	69	0.9732	39.88	14.28571	5.28
M05	Männikjärve	5	15.8	69	0.9155	42.13	11.0119	4.76

Abbreviations: DOC, dissolved organic carbon; DTN, dissolved total nitrogen; JAA Prec, mean precipitations of June, July and August; JAA Temp, mean temperatures of June, July and August; VP cover, vegetation cover.

TABLE A2 Characteristics of the primers targeting the *23S rRNA* gene.

Primers	Forward	Reverse
Sequence	5′-ggattagatacccydgtagtcc-3′	5′-cagcctgttatccctagag-3′
Tm (°C)	59.2	57.0
GC (%)	50	52.6
Nucleotides	22	19
Degeneracy	6	0
Repetition of Gs or Cs longer than 3 bases	No	No
Self-dimer	No	Yes
Cross dimer	No	
Amplicon length	∼160 pb	
Ref	This study	(Sherwood & Presting, 2007)

TABLE A3 Polymerase chain reaction (PCR) reaction conditions for 23S rRNA, *cbbL* and *bchY* genes.

Gene targeted	23S rRNA gene	*bchY* gene	*cbbL* gene
Annealing temperature	55°C	50°C	52°C
PCR conditions	95°C—10 min	95°C—10 min	95°C—10 min
	35 cycles	45 cycles	38 cycles
	94°C—60 s	94°C—60 s	94°C—60 s
	55°C—45 s	50°C—45 s	52°C—30 s
	72°C—45 s	72°C—60 s	72°C—60 s
	72°C—10 min	72°C—10 min	72°C—10 min

TABLE A4 Results of ANOVA and posthoc test for comparison of *16S rRNA* gene concentration between depths in Counozouls and Männikjärve.

Depth	Counozouls	Männikjärve
D1–D2	$p = 0.029$	$p = 0.942$
D1–D3	$p = 6.5 \times 10^{-5}$	$p = 0.176$
D2–D3	$p = 0.0082$	$p = 0.287$

TABLE A5 Results of ANOVA and posthoc test for comparison of *23S rRNA* gene concentration between depths in Counozouls and Männikjärve.

Depth	Counozouls	Männikjärve
D1–D2	$p = 0.189$	$p = 3.3 \times 10^{-4}$
D1–D3	$p = 0.624$	$p = 4 \times 10^{-7}$
D2–D3	$p = 0.038$	$p = 4.9 \times 10^{-4}$

TABLE A6 Results of ANOVA and posthoc test for comparison of *cbbL* gene concentration between depths in Counozouls and Männikjärve.

Depth	Counozouls	Männikjärve
D1–D2	$p = 0.042$	$p = 0.789$
D1–D3	$p = 0.0014$	$p = 2.1 \times 10^{-4}$
D2–D3	$p = 0.175$	$p = 6.1 \times 10^{-4}$

TABLE A7 Results of ANOVA and post-hoc test for comparison of *pufM* gene concentration between depths in Counozouls and Männikjärve.

Depth	Counozouls	Männikjärve
D1–D2	$p = 0.415$	$p = 0.065$
D1–D3	$p = 0.063$	$p = 3.1 \times 10^{-5}$
D2–D3	$p = 0.463$	$p = 0.0015$

TABLE A8 Results of linear mixed-effects models in which 16S rRNA, 23S rRNA, *cbbL* and *pufM* genes abundance were explained by a combination of pH, nutrients, climate and vegetation parameters.

	16S rRNA gene		23S rRNA gene		*cbbL* gene		*pufM* gene	
Parameters	***F*-value**	***p*-value**	***F*-value**	***p*-value**	***F*-value**	***p*-value**	***F*-value**	***p*-value**
pH	2.673	0.163	8.282	0.034	16.898	0.0093	8.664	0.0321
Nutrient	0.829	0.404	0.000028	0.996	0.166	0.701	0.00433	0.9501
Climate and vegetation	9.654	0.027	11.749	0.019	8.962	0.0303	7.205	0.0436

Note: Nutrients included dissolved organic carbon and dissolved total nitrogen, climate and vegetation included June, July and August temperatures, precipitations and vegetation cover. The experimental sites were considered as a random effect.